Resistivity Depends on Preferred Orientation for Transparent Conductive Thin Films

Ligang Ma*

School of Electronic Engineering, Nanjing Xiaozhuang University, Nanjing 211171, China

Xiaoqian Ai

College of Physics and Electronic Engineering, Jiangsu Second Normal University, Nanjing 210013, China

Hanzhi Quan, Wei Yang and Xingxing Du

School of Electronic Engineering, Nanjing Xiaozhuang University, Nanjing 211171, China

An Al-doped ZnO (AZO) thin film is an important and useful material for optoelectronic devices. In this paper, pure ZnO and AZO thin films were deposited on glass substrates by using pulsed laser deposition (PLD) at different substrate temperatures from room temperature to 650°C. The effect of substrate temperature on the crystallization behavior and optoelectronic properties of the AZO thin films were studied using X-ray diffraction (XRD), atomic force microscopy (AFM), transmittance spectra and resistance measuring system, and so on. The XRD results indicated that all the samples were polycrystalline with a hexagonal wurtzite structure. As the substrate temperature was increased from RT to 650°C, the preferred orientation of the AZO thin films undergone a gradual change that affect the resistivity of the thin film. The AFM morphology also showed the same growth pattern. The average optical transmittance of over 90% in the visible range was obtained at a substrate temperature of 400°C. In addition, with increasing substrate temperature, the optical band gap decreased first and then increased, reaching a minimum at 400°C, which is the same trend as the resistivity. These results indicate that the atoms can easily diffuse from one position to another at the proper substrate temperature. The atoms trapped in non-equilibrium positions can shift to positions closer to equilibrium, which causes the Al atoms to be evenly disperse on the surface of the ZnO thin film to improve the transmittance and the conductivity.

I. INTRODUCTION

In the past few years, ZnO thin films have attracted much attention for their potential optoelectronic applications, such as transparent conductive contacts [1], solar cells [2], laser diodes [3], ultraviolet lasers [4], thin film transistors [5], and light emitting diodes [6]. This is attributed to their having a wide direct band gap (3.37 eV) and large excition binding energy (60 mV) at room temperature [7]. As is well known, optical transmittance of a pure ZnO thin film is over 95% in the visible range, but the drawback is that it has a high resistance. Because of this, ZnO thin films cannot be used as window electrodes for optoelectronic devices and can cause a large series resistance in photoelectric devices. Therefore, for pure ZnO thin films, some properties, such as their optical and electrical performances, are often poor [8], which must be changed through an external method.

Doping provides a very effective method to modify and improve the electrical and optical properties of pure thin films [9]. Recently, many elements, such as Cu [10], Ti [11], Mg [7], Co [12], and Al [13], have been doped into or alloyed with ZnO thin film, and good properties have been obtained for on all kinds of devices. Among the various types of doped ZnO films, Al is a very good dopant due to its low cost, non-toxicity, and high stability in the visible wavelength region. Due to these unique properties, Al-doped ZnO thin films (AZO) have been widely studied and successfully applied in many fields.

Several deposition techniques, such as RF sputtering [14], atomic layer deposition [15], reactive evaporation [16], and pulsed laser deposition method (PLD) [17] and

*E-mail: maligang186@163.com

so on, have been used for growing AZO thin films. In comparison with other techniques, the composition of the films grown by using PLD is quite close to that of the target [18]. In addition, due to the high kinetic energies (> 1 eV) of the atoms in laser-produced plasmas, thin films are usually grown at low temperatures or room temperature [18,19]. However, at all the growth parameters, the substrate temperature is one of the key factors affecting the crystallization quality of the AZO film. If AZO thin films with high crystal quality and good optoelectronic performance are to be obtained, the effects of substrate temperature at the growth of AZO thin films by using PLD must be clarified.

In this research, pure and AZO thin films were deposited on glass substrates by using PLD at different substrate temperatures. The effect of substrate temperature on the structural and the optical properties of AZO thin films was systematically investigated by using X-ray diffraction (XRD), atomic force microscopy (AFM), transmittance spectra and resistance measuring system, and so on. Finally, we discuss the influence of substrate temperature on the electrical properties of the AZO thin films.

II. EXPERIMENTS

AZO thin films were deposited on glass substrates by using PLD at different substrate temperatures from RT to 650°C. The PLD apparatus were equipped with a KrF excimer laser (wavelength: 248 nm, frequency: 10 Hz). The laser beam was focused by using a lens, and the energy density of the laser beam at the target surface was maintained at 1 J/cm^2. The distance between the target and the substrate was 50 mm. The laser beam was scanned across the surface of the target by using a computer-controlled mirror while the target was rotated. The homemade target with 97 wt.% ZnO and 3 wt.% Al$_2$O$_3$ was 30 mm diameter, 10 mm thick sintered oxide ceramic disk. Before being introduced into the deposition system, the glass substrates were ultrasonically cleaned with acetone and alcohol in sequence for 10 min each, rinsed with distilled water, and dried in nitrogen. The vacuum chamber was evacuated using a turbomolecular pump to a base pressure of 6×10^{-4} Pa. During deposition, high purity Ar and O$_2$ were introduced into the chamber to maintain a pressure of 1.0 Pa for 30 min; the O$_2$:Ar ratio was 10 sccm:10 sccm. The AZO target was pre-shot with the laser in pure Ar for 10 min to remove surface contamination. The substrate was rotated during the growth in order to ensure the uniformity of the thin film. Finally, all thin films were annealed in O$_2$ for 30 min. According to X-ray photoelectron spectroscopy (XPS) results, the Al doping concentration in the AZO thin films, regardless of different substrate temperature, was 0.96 ± 0.08 at.%

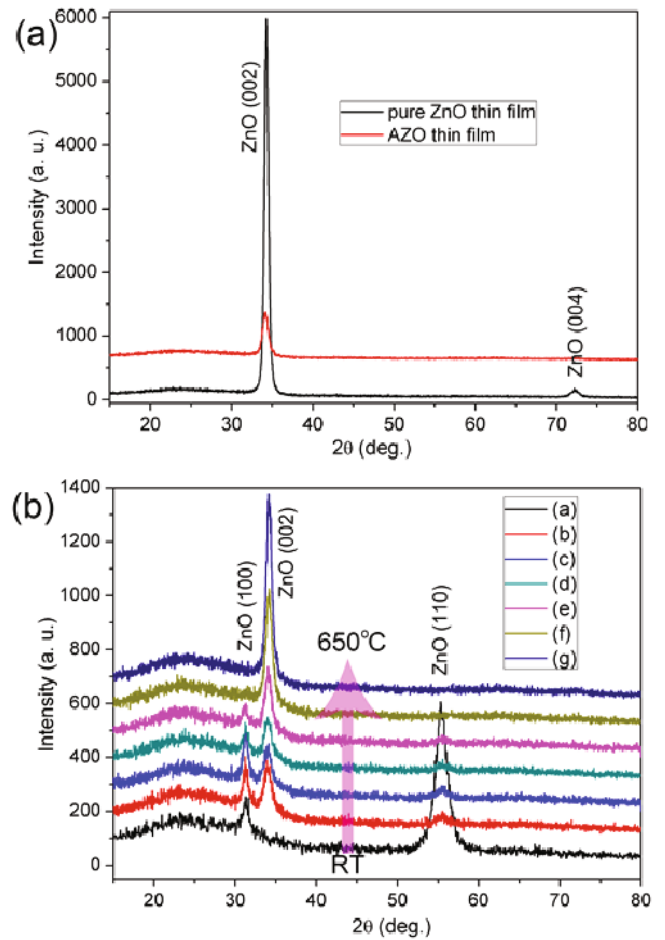The crystal structures were studied by using XRD

Fig. 1. (Color online) (a) XRD diffraction patterns for a pure ZnO thin film (black line) and an AZO thin film (red line) deposited at a substrate temperature of 650°C on glass substrates. (b) XRD diffraction patterns for AZO thin films deposited at substrate temperatures of (a) RT, (b) 300, (c) 350, (d) 400, (e) 450, (f) 550, and (g) 650°C.

(Rigaku) with Cu Kα radiation ($\lambda = 0.15406$ nm) in the range of 15–80°. The operating voltage and current were maintained at 40 kV and 60 mA, respectively. The surface morphology of thin films was observed using AFM (Bruker, MultiMode). The absorption and transmittance spectra of the AZO thin films were obtained by a UV-vis spectrophotometry (UV-3600). The electronic properties were measured by using a home-assembled transport measurement system with a Keithley 2400 Source Meter. All of the measurements were performed at room temperature.

III. RESULTS AND DISCUSSION

In order to reveal the effect of the Al dopant on the pure ZnO thin film, we measured the XRD diffraction patterns of a pure ZnO film and an AZO thin film grown

Table 1. The unit cell parameters of pure ZnO thin film and AZO thin films calculated from XRD patterns at different substrate temperature.

Sample	2θ (°)	FWHM (°)	d_{002} (nm)	c (nm)	D (nm)
Pure ZnO	34.26	0.539	0.2615	0.5230	15.4
(a) RT	–	–	–	–	–
(b) 300°C	33.90	0.862	0.2642	0.5284	9.6
(c) 350°C	34.0	0.822	0.2634	0.5268	10.1
(d) 400°C	34.04	0.759	0.2632	0.5264	10.9
(e) 450°C	34.08	0.759	0.2629	0.5258	11.0
(f) 550°C	34.16	0.707	0.2623	0.5246	11.8
(g) 650°C	34.20	0.659	0.2620	0.5240	12.6

Table 2. Texture coefficient C_i and the preferred orientation factor for a pure ZnO thin film and for AZO thin films deposited at various the substrate temperatures.

	C_i (100)	C_i (002)	C_i (110)	C_i (004)	f
Pure ZnO	0	3.7	0.006	0.27	1.57
(a) RT	0.79	0	3.21	0	1.3
(b) 300°C	2.23	1.26	0.5	0	0.8
(c) 350°C	1.92	1.65	0.42	0	0.81
(d) 400°C	1.41	2.16	0.42	0	0.84
(e) 450°C	0.82	2.92	0.24	0	1.15
(f) 550°C	0.26	3.74	0	0	1.58
(g) 650°C	0.14	3.86	0	0	1.65

under the same conditions, and the results are shown in Fig. 1(a). Clearly the crystallization quality of ZnO thin film was affect by the Al dopant. A pronounced diffraction peak and a weak diffraction peak were observed at $2\theta = 34.26°$, and $72.22°$, which were attributed to the (002) and the (004) planes of the ZnO phase, respectively. This result showed that both samples were polycrystalline with a structure that belonged to the ZnO hexagonal wurtzite structure. And, these two thin films had preferential orientations along the c-axis. The intensity of the (002) diffraction peak decreased and the (004) diffraction peak disappeared due to Al doping. In addition, the full widths at half maximum (FWHM) of the (002) diffraction peaks were found to be increased after Al doping. This indicates that the orientation of the ZnO thin film was strongly affected by Al-doping and that the crystallization quality of the ZnO thin film was poor after Al doping.

According to the Bragg formula [20], the crystalline plane distance d_{002} and d_{100} can be written as

$$d = \frac{\lambda}{2\sin\theta}, \qquad (1)$$

where λ and θ are the X-ray wavelength (0.1541 nm) and the diffraction angle of the peak. For a hexagonal wurtzite structure, the lattice constants a and c can be calculated by using the following formula [21]:

$$d_{hkl} = \left(\frac{4}{3}\frac{h^2 + hk + k^2}{a^2} + \frac{l^2}{c^2}\right)^{-1/2}. \qquad (2)$$

The indices (h, k, l) are the Miller indices. The parameter d_{hkl} denotes the crystalline plane distance for indices (h, k, l). The values of these parameters are shown in Table 1. From Table 1, the lattice constant c of the Al-doped ZnO thin film is larger than that of the pure ZnO thin film. Two doped forms of elemental Al are present in ZnO films, interstitial atoms and substitute atoms. The radius of Al^{3+} and Zn^{2+} ions are 0.053 and 0074 nm, respectively. If Al^{3+} replaces Zn^{2+} to form the AZO thin film, the lattice constant c becomes smaller. On the contrary, if Al exists as an interstitial atom between the lattices of ZnO, the lattice is expected to be
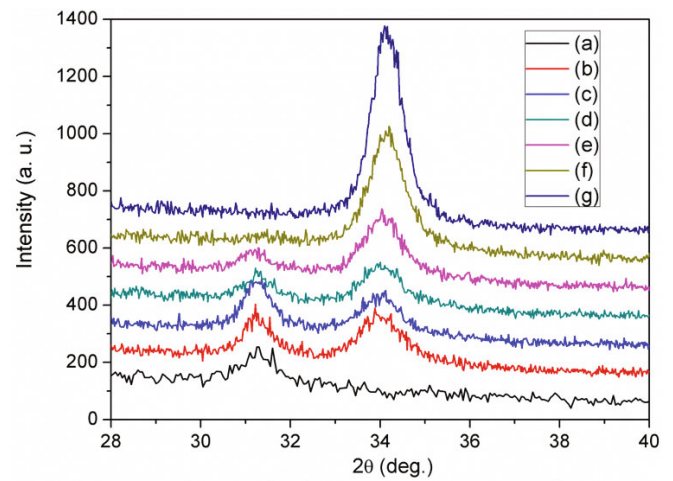

Fig. 2. (Color online) Enlarged XRD patterns between 28° and 40° for AZO thin films deposited at substrate temperatures of (a) RT, (b) 300, (c) 350, (d) 400, (e) 450, (f) 550, and (g) 650°C.

larger. Therefore, Al^{3+} ions were doped in the lattice of ZnO as interstitial atoms in our experiment, which resulted in an increase in the lattice constant and the (002) crystalline plane distance, which would result in a decreased diffraction angle compared with the pure ZnO thin film.

The influence of substrate temperature on the crystallization behavior was also characterized by using XRD. Figure 1(b) shows XRD patterns of AZO thin films prepared at various substrate temperatures. Three main diffraction peaks match those of the hexagonal wurtzite-type ZnO thin film, and correspond to the (110), (002) and (110) planes of the ZnO phase, respectively. As shown in Fig. 1(b), the crystal microstructure obviously depends on the substrate temperature. Initially, the relative intensity of the (100) diffraction peak was weaker than that of the (110) diffraction peak, and the (002) diffraction peak was not found in the XRD pattern. As the substrate temperature was increased, the XRD pattern underwent a gradual change. The (100) diffraction
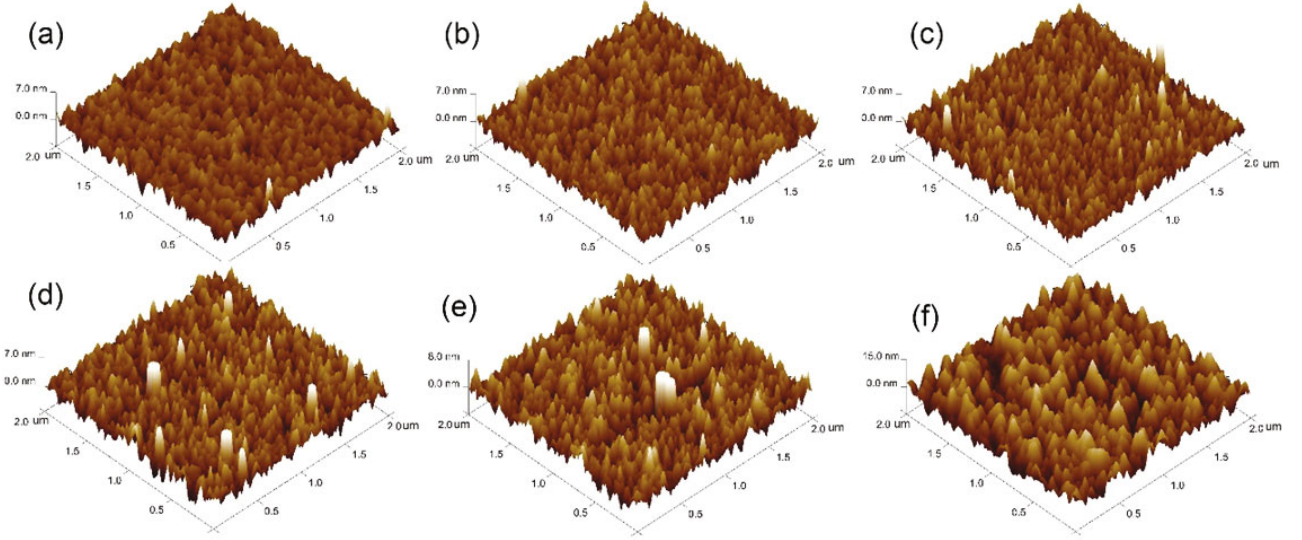
Fig. 3. (Color online) AFM images of AZO thin film deposited at various substrate temperatures: (a) RT, (b) 300, (c) 400, (d) 450, (e) 550, and (f) 650°C.

peak became weak and finally disappeared at a substrate temperature of 400°C. Meanwhile, the (002) diffraction peak appeared and its intensity increased. This can be clearly seen in the enlarged XRD patterns between 28–40° (Fig. 2).

The crystallite size was also calculated using the Scherrer equation [23]:

$$D = \frac{0.9\lambda}{\beta \cos\theta},\tag{3}$$

where λ, θ and β are the X-ray wavelength (0.15406 nm), diffraction angle and FWHM of the ZnO film (002) peak. The calculation results for the (100) and the (002) diffraction peaks of AZO thin films at various substrate temperature are presented in Table 1. The FWHM of the (002) diffraction for the AZO thin film gradually decreased and the crystallite size grew with increasing substrate temperature, which means that the crystal quality of the AZO film improved with increasing substrate temperature.

To analyze the preferential orientation of each sample as a whole, we calculated the texture coefficient C_i and the preferred orientation factor f of AZO thin film by using [22]:

$$C_i = \frac{I_i/I_{0i}}{(1/N)\sum_{i=1}^{N}(I_i/I_{0i})},\tag{4}$$

$$f = \sqrt{\frac{\sum_{i=1}^{N}(C_i - 1)^2}{N}},\tag{5}$$

where I_i is the intensity of a generic peak in the XRD pattern, I_{0i} is the intensity of a generic peak for a completely random sample (JCPDS card No. 36-1451), and N is the number of reflections considered in the analysis.

We considered four main diffraction peaks. The texture coefficients and the preferred orientation factors f for all samples are listed in Table 2. Values of f are used to compare the degree of orientations between samples. If f equals 0, the grain orientation of a film is the same as that of the standard powders. Therefore, the f value indicates the preferred orientation level of AZO thin film samples. Clearly from Table 2, the preferred orientation is along the (110) direction for growth at RT. With increasing substrate temperature, the preferred orientation of the AZO thin film is first along the (100) direction and then along the (002) direction. As the substrate temperature continued to increase, the c-axis orientation became stronger.

A typical morphological evolution of an AZO thin film with substrate temperatures is shown in Fig. 3. The substrate temperature was found to have a great influence on the surface structure of the thin film. From the AFM images, the grain boundaries for the AZO thin film prepared at RT are blurred, and the morphology was found to be continuous and dense, which indicated that the thin film had grew parallel to the substrate. With increasing substrate temperature, the thin film exhibited columnar morphology. We presume that high substrate temperatures provided energy, enabling atoms to migrate and grow along the c-axis. The grain size evidently became larger with increasing substrate temperature, which is consistent with the results of the Scherrer equation. The root mean squares of the average surface roughnesses of the AZO thin film were 1.05, 1.16, 1.3, 1.39, 1.77, 2.29, and 3.67 nm, respectively. Apparently, an increase in the substrate temperature caused an increase in the surface roughness.

As is well known, the optical properties of ZnO thin film can be improved by Al doping. Figure 4 shows the
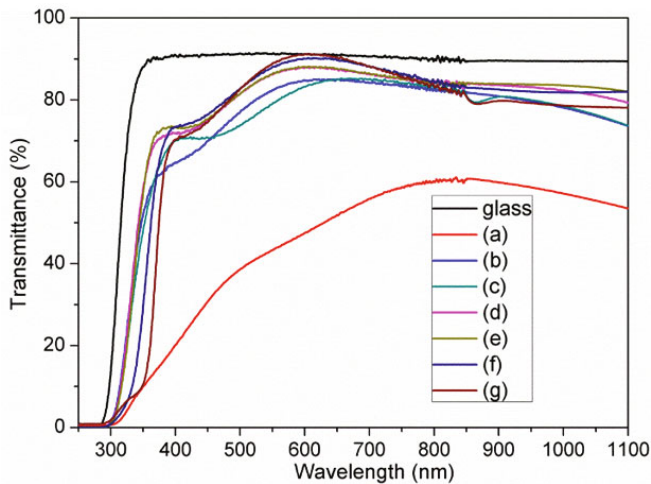
Fig. 4. (Color online) Transmittance spectra of AZO thin films prepared at (a) RT, (b) 300, (c) 400, (d), 450, (e) 550, and (f) 650°C. The black line shown in the figure belongs to the transmittance spectrum for the glass substrate.

Fig. 5. (Color online) Plot of $(\alpha h v)^2$ *vs.* $h v$ for AZO thin films deposited at various substrates temperatures: (a) RT, (b) 300, (c) 400, (d), 450, (e) 550, and (f) 650°C. Inset: partial enlarged patterns of (b), (c), (d), and (e).

optical transmission spectra of AZO thin films grown at various substrate temperatures. As for AZO grown at RT, the transmittance is very low, and no obvious absorption edge is seen. This is because the kinetics is relatively small, and atoms are hardly the interstitial positions. The transmittance was larger when the substrate temperature was above 300°C, and the average optical transmittance in the visible region was found to be in the range of 80%. The transmittance is almost the same as that of the glass substrate near a wavelength of 600 nm. In addition, absorption edges were seen in the AZO thin film at about 350 nm, which corresponded to the optical band gap of the ZnO thin film. The absorption edge shifted to a shorter wave length (blue shift) first and then to a longer wave length as the substrate temperature was increased. Obviously, the AZO thin film prepared at 550°C exhibited better transparency.

The optical band gap of the AZO thin films was determined from the absorption spectra by using the Tauc relationship as follows [24]:

$$\alpha h v = A(h v - E_g)^{1/2} \tag{6}$$

where α is the absorption coefficient, h is Plancks constant, v is the photon frequency, A is constant, and E_g is the optical band gap. Figure 5 shows plots of $(\alpha h v)^2$ as a function of photon energy hv for AZO thin films grown at various substrate temperature. The straight-line portion of the curve, when extrapolated to zero, gives the optical band gap. From the results of Fig. 5, the optical band gap is found to decrease first and then to increase, reaching a minimum of about 3.69 eV at 400°C. In addition, the Tauc plots for AZO thin films prepared at high temperature (650°C) have two linear parts because there are large holes in the thin film, which can be clearly seen in the AFM images.
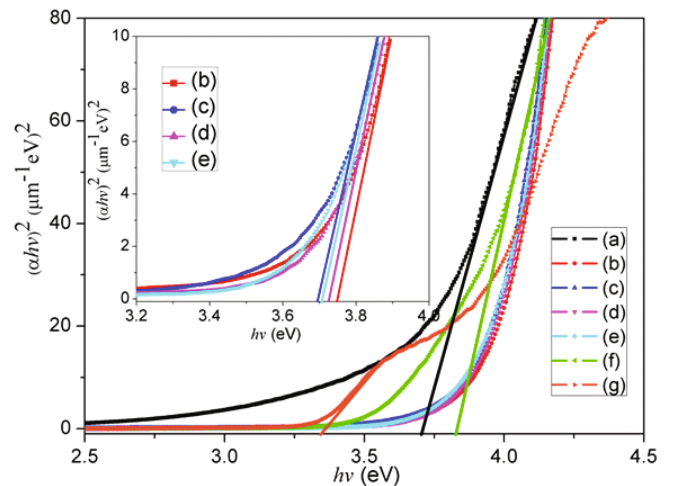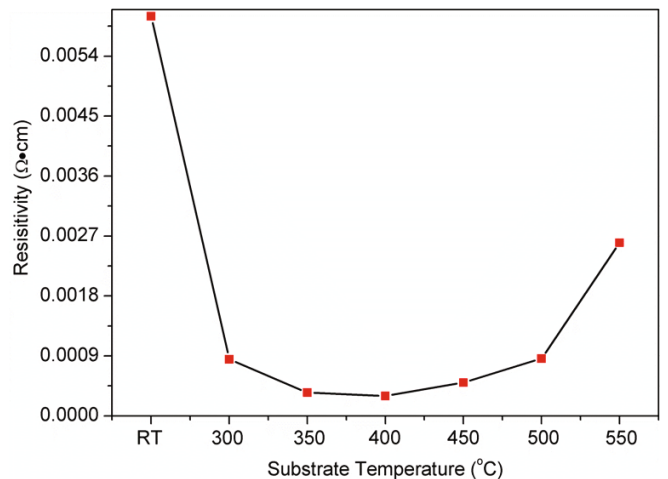

Fig. 6. (Color online) Resistivity of AZO thin films deposited at various substrates temperatures.

The room-temperature resistivities for all thin films were measured, and the results are shown in Fig. 6. The resistivity of the AZO thin film is seen to decrease first and then to increase, reaching a minimum at 400°C. The conductivity of the ZnO thin film has improved for two reasons. On the one hand, the micro-metal Al-doping of the ZnO thin films can improve the conductivity of the thin films. On the other hand, at the proper substrate temperature, the mobility of the atoms in the thin film is greatly increased. Thus, the atoms can easily diffuse from one position to another. Then, the atoms trapped in non-equilibrium positions can shift to positions closer to equilibrium, which causes the Al atoms to be evenly dispersed on the surface of the ZnO thin film. At high temperature, the meal Al atoms fuse, which leads to higher resistivity.

IV. CONCLUSION

In this research, AZO thin films were deposited on glass substrates by using PLD at different substrate temperatures. The crystal structure, surface morphology, transmittance and electrical characteristics of the AZO were strongly aected by the substrate temperature. XRD measurements revealed that the sample deposited at RT grew in the (110) direction, while the preferred orientation of the AZO thin film changed toward the (100) and the (002) directions as the substrate temperature was increased. In addition, an increase in the substrate temperature caused an increase in the roughness. Finally, we studied the influence of the substrate temperature on the optical and the electrical properties of AZO thin films. AZO thin films with high transmittance and low resistivity were obtained at a substrate temperature of 400°C. This research may be useful in the field of transparent electrodes.

ACKNOWLEDGMENTS

REFERENCES

[1] K. Tang *et al.*, Appl. Surf. Sci. **433**, 177 (2018).
[2] I. Seo and S. O. Ryu, J. Korean Phys. Soc. **66**, 790 (2015).
[3] Ü. Özgür *et al.*, J. Appl. Physics. **98**, 041301 (2005).
[4] S. Chu *et al.*, Appl. Phys. Lett. **93**, 181106 (2008).
[5] B. S. Ong, C. Li, Y. Li, Y. Wu and R. Loutfy, J. Am. Chem. Soc. **129**, 2750 (2007).
[6] J. H. Lim *et al.*, Adv. Mater. **18**, 2720 (2010).
[7] C. Q. Cai, H. Q. Zhang, J. Xie and L. G. Ma, J. Korean Phys. Soc. **70**, 856 (2017).
[8] S. K. Singh and R. Singhal, Thin Solid Films **653**, 377 (2018).
[9] L. Ma, X. Ai and X. Wu, J. Alloy. Compd. **691**, 399 (2017).
[10] L. Ma *et al.*, Appl. Surf. Sci. **257**, 10036 (2011).
[11] L. G. Ma, X. Q. Ai, X. L. Huang and S. Y. Ma, Superlattice. Microst. **50**, 703 (2011).
[12] G. Nam *et al.*, J. Korean Phys. Soc. **63**, 1962 (2013).
[13] M. Mickan *et al.*, J. Phys. Chem. C **121**, 14426 (2017).
[14] L. L. Yue *et al.*, J. Korean Phys. Soc. **68**, 686 (2016).
[15] İ. Orak, Solid State Commun. **247**, 17 (2016).
[16] G. Gordillo, A. A. R. Botero and E. A. Ramirez, J. Mater. Res. Technol. **5**, 219 (2016).
[17] A. Taabouche *et al.*, Ceram. Int. **42**, 6701 (2016).
[18] Y. Liu, L. Zhao and J. Lian, Vacuum **81**, 18 (2006).
[19] L. Zhao *et al.*, Appl. Surf. Sci. **252**, 8451 (2006).
[20] G. Sanon, R. Rup and A. Mansingh, Thin Solid Films **190**, 287 (1990).
[21] G. J. Fang, D. J. Li and B. L. Yao, Phys. Status Solidi **193**, 139 (2002).
[22] M. F. Mendoza *et al.*, Sol. Energ. Mat. Sol. C **95**, 2023 (2011).
[23] T. Yamada *et al.*, Surf. Coat. Tech. **202**, 973 (2007).
[24] M. Girtan and G. Folcher, Surf. Coat. Tech. **172**, 242 (2003).